

# SIMULATION OF MODELS FOR THE GLASS TRANSITION: IS THERE PROGRESS?

Kurt Binder<sup>1</sup>, Jörg Baschnagel<sup>2</sup>, Walter Kob<sup>3</sup>, and Wolfgang Paul<sup>1</sup>

<sup>1</sup> Institut für Physik, Johannes-Gutenberg-Universität Mainz, D-55099 Mainz, Germany

<sup>2</sup> Institut Charles Sadron, Université Louis Pasteur, 6, rue Bossingault, F-67083 Strasbourg, France

<sup>3</sup> Laboratoire des Verres, Université Montpellier II, F-34095 Montpellier, France

**Abstract.** The glass transition of supercooled fluids is a particular challenge for computer simulation, because the (longest) relaxation times increase by about 15 decades upon approaching the transition temperature  $T_g$ . Brute-force molecular dynamics simulations, as presented here for molten  $\text{SiO}_2$  and coarse-grained bead-spring models of polymer chains, can yield very useful insight about the first few decades of this slowing down. Hence this allows to access the temperature range around  $T_c$  of the so-called mode coupling theory, whereas the dynamics around the experimental glass transition is completely out of reach. While methods such as “parallel tempering” improve the situation somewhat, a method that allows to span a significant part of the region  $T_g \leq T \leq T_c$  is still lacking. Only for abstract models such as the infinite range 10-state Potts glass with a few hundred spins this region can be explored. However this model suffers from very strong finite size effects thus making it difficult to extrapolate the results obtained for the finite system sizes to the thermodynamic limit.

For the case of polymer melts, two different strategies to use lattice models instead of continuum models are discussed: In the first approach, a mapping of an atomistically realistic model of polyethylene to the bond fluctuation model with suitable effective potentials and a temperature-dependent time rescaling factor is attempted. In the second approach, devoted to a test of the entropy theory, moves that are artificial but which lead to a faster relaxation (“slithering snake” algorithm) are used, to get at least static properties at somewhat lower temperatures than possible with a “realistic” dynamics. The merits and shortcomings of all these approaches are discussed.

## 1 Introduction

The reason for the slowing down of the dynamics of supercooled liquids and the resulting glass transition to an amorphous solid is one of the biggest unsolved problems in the physics of condensed matter [1,2,3,4,5] and it is also a particular challenge for computer simulation [6,7,8,9,10,11,12]. The present introductory section intends to remind the reader on the main experimental facts and some theoretical ideas about the glass transition, and will also serve to make clear why in this problem there exists a gap of time-scales that simulations need to bridge.

As is well known, it is already a problem to characterize the static structure of a glass: the structure of an amorphous material is not regular like a crystalline solid, but shows only short range order similar to a liquid. However, the latter flows, while the amorphous solid is rigid! In fact, if one makes a scattering experiment, it is hard to distinguish from the structure whether one has a fluid above the glass transition temperature  $T_g$  or a solid below  $T_g$  (Fig. 1) [13,14]. If one approaches  $T_g$ , the structural relaxation time  $\tau$  which is related to the viscosity  $\eta(T)$ , for instance - increases smoothly by up to 15 decades, as shown schematically in Fig. 2, without any accompanying significant structural change detectable by scattering experiments (Fig. 1). This increase of  $\eta(T)$  is often fitted to the Vogel-Fulcher relation [1]

$$\eta(T) \propto \exp[E_{VF}/(T - T_{VF})], \quad (1)$$

where  $E_{VF}$  is an effective activation barrier. From this functional form it is clear that  $\eta(T)$  is predicted to diverge at the Vogel-Fulcher temperature  $T_{VF}$ , which is lower than  $T_g$ , of course, if one invokes the empirical definition of  $T_g$  via  $\eta(T = T_g) = 10^{13}$  Poise [1]. However, it is questionable whether the temperature dependence of  $\eta$  as given by Eq. (1) really holds.

Another very common relation often used to describe various relaxation functions of glassforming fluids is the Kohlrausch-Williams-Watts function, also called stretched exponential, [1],

$$\varphi(t) \propto \exp[-(t/\tau)^\beta]. \quad (2)$$

This relation involves an exponent  $\beta \leq 1$ , whose precise physical significance is somewhat obscure. Again it is unknown under which circumstances (if any) Eq. (2) is exact, and in which it is just a convenient fitting formula to represent data.

Often it is claimed that the glass transition is a purely kinetic phenomenon, and if one would be able to wait long enough (which could mean times like the age of the universe, however!) one could see that glass is not really a solid but still a fluid that flows. However, this idea is not generally accepted, since there are some indications that there may be an underlying quasi-equilibrium phase transition between metastable phases, namely from the supercooled metastable fluid to an (also metastable) ideal glass phase (the stable phase for temperatures lower than the melting temperature  $T_m$  is of course the crystal). Such an indication is Kauzmann's entropy paradox [15]: By studying the difference in entropy between liquid and crystal one finds that near  $T_g$  the difference  $\Delta S(T) = S_{\text{fluid}} - S_{\text{crystal}}$  has decreased to about 1/3 of its value  $S_m$  at the melting/crystallization temperature  $T_m$ . If this trend is extrapolated (linearly in  $T$ ) to even lower temperatures,  $\Delta S(T)$  would become negative below the Kauzmann temperature  $T_0$  (which is usually quite close to the Vogel-Fulcher-temperature  $T_{VF}$ ), see Fig. 2. It would indeed be paradox if the entropy of the supercooled fluid (with its disordered structure) were less than the entropy of the ordered solid! One possibility to bypass the problem is to assume that this "entropy catastrophe" is avoided by a phase transition at  $T_0$  (or at some temperature in between  $T_0$  and  $T_g$ ). In fact,

for the glass transition of polymer melts Gibbs and Di Marzio [17] proposed an approximate theory that shows such a vanishing of the entropy at  $T_0$ , and subsequently Adam and Gibbs [18] suggested arguments to show that Eq. (1) holds with  $T_{VF} = T_0$ . However, although these concepts enjoy some popularity, all these arguments are based on very crude and hardly justifiable assumptions and approximations, and hence they are not accepted by many researchers. For instance, the mode coupling theory of the glass transition (MCT)[3] claims that there is indeed an underlying transition but this is *not* a phase transition in the sense of thermodynamics but rather a “dynamical transition” from an ergodic to a nonergodic behavior. This transition should occur at a critical temperature  $T_c$  and can be seen in the form of the time dependence of the correlation function of density fluctuations or its Fourier transform  $\Phi_q(T)$ , see Fig. 2. Above  $T_c$ , this correlator decays to zero, but as  $T_c$  is approached a plateau develops whose “lifetime” gets larger and larger until it diverges, in the ideal case: the system gets “stuck”, the decay of  $\Phi_q(t)$  stops at the “nonergodicity parameter”  $f_c$ , an order parameter for the glass transition that appears discontinuously at  $T_c$ . The physical idea behind this theory is the “cage picture”: the motion of any atom in a dense fluid is constrained by its neighbors, which form a cage around it. At low enough temperatures the escape out of the cage gets blocked. MCT predicts that close to this dynamical transition  $\tau$  and  $\eta(T)$  show a power-law divergence as one approaches  $T_c$ ,

$$\tau \propto \eta(T) \propto (T - T_c)^{-\gamma}. \quad (3)$$

In reality this dependence is, however, observed only in a limited temperature interval. The way out of this dilemma is the argument that one must not neglect (as “idealized” mode coupling theory does [3]) thermally activated processes, so-called “hopping processes”, by which atoms supposedly can escape from their cage when  $T$  is less than  $T_c$ . The theory then claims [19] that a simple Arrhenius behavior results in this region,  $\log \tau \propto 1/T$  for  $T < T_c$ , and in the vicinity of  $T_c$  the power-law divergence of Eq. (3) is rounded off to a smooth crossover from the power law to the Arrhenius divergence. Thus this theory does not involve any phase transition, there is just a smooth crossover from one type of dynamical behavior to another one near  $T_c$ , and  $T_g$  means that relaxation times have grown so large that the system falls out of equilibrium.

In real systems this crossover seems to occur at a viscosity somewhere between 10 and  $10^3$  Poise, i.e. a time window that can be explored with molecular dynamics (MD) simulations. Hence such simulations are able to investigate the beginning of the approach to the critical temperature  $T_c$  which MCT describes [3] and hence are very useful to check the validity of this theory. However, the following 10 decades of the viscosity between  $T_c$  and  $T_g$  are out of reach for MD simulations so far. Unfortunately this is precisely the region that one needs to explore, for a definite distinction between the theories!

Thus although straightforward atomistic MD methods [20,21] clearly face a dilemma, we shall nevertheless describe how far one can push this type of approach, choosing  $\text{SiO}_2$  as an example (Sec. 2). A method to extend the range of

times and accessible temperatures somewhat is the concept of “parallel tempering” [22,23,24,25,26], and this approach and its problems will be presented in Sec. 3. For the sake of contrast, Sec. 4 will then describe the 10-state Potts glass model. Although this model is only an abstract caricature for a real glass, it has the merit that quite a few results are known analytically and that Monte Carlo simulations are possible at  $T_c$  and even at lower temperatures, if one considers only systems of a few hundred Potts spins. The disappointing aspect is, Sec. 4, that even in this very idealized case one learns relatively little about the glass transition of the infinite system, since one has to fight against dramatic finite size effects [27,28,29,30]!

Then we shall describe briefly (Sec. 5) a coarse-grained model of short polymer chains [14,31,32,33,34,35,36,37]. This bead-spring model is quite successful in reproducing a number of experimental results qualitatively, as already exemplified in Fig. 1. The cooling rates that one can reach are about 3 orders of magnitude smaller than for  $\text{SiO}_2$ . Thus the model is very useful for testing mode coupling theory [36,37]. However, also for this system there is actually only a dim hope that one can get distinctly below the critical temperature  $T_c$ ! With respect to that it may be better to work with the so-called bond fluctuation model on the lattice [6,38,39,40,41,42,43,44,45,46,47] - a system which allows to equilibrate melts at low temperatures with artificial moves [44,45,46,47]. By simulations of this model also the configurational entropy and its temperature dependence can be extracted [44,45] and thus it can be shown that the entropy theory of Gibbs and Di Marzio [17] is rather inaccurate and misleading (Sec. 6). Finally, an interesting variant (Sec. 7) of the bond fluctuation model will be considered. Here one uses effective potentials that are constructed such that a real material is mimicked, e.g. polyethylene [48]. This trick allows that part of the problem of bridging the time scales is taken care of by a “time rescaling factor” [48], a special translation factor between the physical time and the Monte Carlo time. Sec. 8 then will summarize some of the conclusions emerging from all this work.

## 2 Towards the simulation of real glassy materials: The case of $\text{SiO}_2$

Molten  $\text{SiO}_2$  is a prototype of a network glassformer. Furthermore it is a system that is well suited for molecular dynamics simulations since a very well-tested pair potential based on quantum-chemical calculation has been developed [49]. By a suitable combination of long-range Coulomb interactions and short range forces, chosen in the form

$$V_{ij}(r) = \frac{q_i q_j e^2}{r} + A_{ij} \exp(-B_{ij} r) - C_{ij}/r^6 \quad \text{with } i, j \in \{\text{Si}, \text{O}\}, \quad (4)$$

the effective interaction between the ions can be described reliably. Here  $e$  is the charge of an electron,  $q_{\text{O}} = -1.2$ ,  $q_{\text{Si}} = 2.4$ , and the values of the parameters

$A_{ij}$ ,  $B_{ij}$  and  $C_{ij}$  can be found in Ref. [49]. This potential is able to describe the formation of covalent bonds without the explicit assumption of three-body forces, whose calculation would be very time consuming. Due to the long range of the electrostatic interactions, Ewald summation techniques have to be used, while the short range part of the potential can be cut off at a suitable radius  $r_c$ . It turns out that  $r_c = 5.5\text{\AA}$  yields good results [50]. The MD time step, however, must be chosen relatively small, namely  $\delta t = 1.6\text{fs}$ . Note that the presence of the long range Coulombic interactions make the calculation of the forces still a quite CPU-intensive task. Furthermore one has to average the results over several independent runs in order to improve the statistics.

In a first set of simulations, the method used to cool the sample was very similar to the procedure used in glass factories where the temperature is reduced linearly with time  $t$ , starting from some initial temperature  $T_i$  such that  $T(t) = T_i - \gamma t$ , where  $\gamma$  is the cooling rate [50]. The main difference between the simulation and the cooling of the real material are the actual numbers used here: The initial temperature that had to be chosen in the simulation was very high,  $T_i = 7000\text{K}$ , and cooling rates were between  $\gamma = 10^{15}\text{K/s}$  and  $\gamma = 10^{12}\text{K/s}$  [50]. In contrast the glass factory uses typical initial temperatures of  $1600\text{K}$  and cooling rates of  $1\text{K/s}$  or even less, so the simulation is at least 12 orders of magnitude off! Despite these extremely high cooling rates - which are inevitable due to the heavy computational burden - the generated structures are qualitatively reasonable. In particular one obtains random tetrahedral networks in which almost all Si atom sit in the center of a tetrahedron and most of the O atoms sit at the corners.

Earlier investigators (for a review see [7,8,50]) were so bold to claim that such glass structures are identical to those occurring in nature, denying any significant dependence on cooling rate. However, as we have shown [50], such a claim is foolish since one sees a pronounced dependence on cooling rate in many quantities, including the structure. As a typical example we show in Fig. 3 how the distribution of the length  $n$  of rings depends on  $\gamma$ [50]. (See the figure caption for a definition of this length.) It is seen that over the range of  $\gamma$  that is accessible there is a significant increase of  $P(n = 6)$  and a significant decrease of  $P(n = 3)$  and  $P(n = 4)$ , while  $P(n = 5)$ ,  $P(n = 7)$  and  $P(n = 8)$  almost stay constant. Clearly an extrapolation of such data to the physically relevant cooling rate  $\gamma = 1\text{K/s}$  is very difficult, and perhaps not yet possible: Perhaps  $P(n = 3)$  and  $P(n = 4)$  are already practically equal to zero for  $\gamma = 1\text{K/s}$  - we don't really know. Even simple quantities, such as the density of the glass at low temperatures, are hard to predict reliably. (This problem is also complicated by the fact that molten  $\text{SiO}_2$  has at relatively high temperatures a density anomaly where the thermal expansion coefficient changes sign.)

A particular dramatic failure with extrapolations to lower values of  $\gamma$  was encountered in an attempt to determine the cooling rate dependence of the glass transition temperature  $T_g(\gamma)$ . As is done in many experimental studies, one can fit a smooth function of temperature to the liquid branch of the enthalpy (where the melt has not yet fallen out of equilibrium) and another smooth function

to the glass branch of the enthalpy, and estimate  $T_g(\gamma)$  from the temperature where these two branches intersect. Fig. 4 shows a plot of  $T_g(\gamma)$  versus  $\gamma$  - note the logarithmic scale for  $\gamma$ ! - for the simulation of  $\text{SiO}_2$ . One sees, first of all, that there is a very strong dependence of  $T_g(\gamma)$  on  $\gamma$ , with  $T_g(\gamma) \approx 4000\text{K}$  for  $\gamma = 10^{15}\text{K/s}$ , while  $T_g(\gamma)$  has decreased down to about  $T_g(\gamma) \approx 2900\text{K}$  for  $\gamma = 10^{13}\text{K/s}$ . In this range of cooling rates, the dependence of  $T_g(\gamma)$  is not linear in  $\log(\gamma)$ . Nonlinear variations of  $T_g(\gamma)$  that are qualitatively similar to those of Fig. 4 have been reported in the experimental literature, too [51], and are typically described by

$$T_g(\gamma) = T_{VF} - B/[\log(\gamma A)] \quad (5)$$

This dependence can be justified by assuming that the fluid falls out of its (metastable) equilibrium when the time constant of the cooling,  $\gamma^{-1}$ , equals the structural relaxation time  $\tau(T)$  at  $T = T_g(\gamma)$ , and by using the Vogel-Fulcher law from Eq. (1) for  $\tau(T)$ ,  $\tau(T) = A \exp[B/(T - T_{VF})]$ . Obviously, Eq. (5) does provide a very good fit to the data of the  $\text{SiO}_2$  simulation, but the resulting  $T_{VF} = 2525\text{K}$  is rather unreasonable: Remember that the *experimental* glass transition temperature is  $T_g \approx 1450\text{K}$ , the melting temperature of crystalline  $\text{SiO}_2$  is around  $2000\text{K}$ , and  $T_{VF}$  should be significantly lower than  $T_m$  and even somewhat below  $T_g$ , cf. Fig. 2. We emphasize here that the failure of the simulation to predict  $T_g(\gamma = 1\text{K/s})$  is not primarily due to the inaccuracy of the pair potential since, as will be explained in detail below, a different analysis of  $\text{SiO}_2$  simulation data yields much more reasonable results. The failure implied by Fig. 4 simply comes from the fact that the 10-1000 picosecond timescale that is basically probed here is too many orders of magnitude off from the time scale relevant for the glass transition and that therefore an extrapolation of the results becomes a insecure undertaking.

A better way to study amorphous silica is to fix density at a reasonable value, for instance the experimental value, and equilibrate the system at a temperature which is as low as possible. Present day simulations can propagate a system of around 8000 ions over a time span of around 20ns which allows for a full equilibration at  $T = 2750\text{K}$  [52]. Longer time are accessible for smaller systems. However, it was found that if one has fewer than  $O(10^3)$  ions the results are plagued with finite size effects [53]. Simulating a large system over this time scale are on the forefront of what is feasible today, and require the use of multi-processor super computers such as CRAY-T3E, making use of a parallelization of the force calculation [52,53,54].

This well-equilibrated melt can then be used as a starting condition for a cooling run at constant density. The advantage of this procedure is that a state at  $T = 2750\text{K}$  at the correct density is much closer in local structure to the real glass, than the structures generated by the procedures described above, and hence the spurious effects of the by far too rapid quench are much less pronounced. This conclusion is corroborated by a comparison of the simulated structure factor with experiment [55], see Fig. 5. Given the fact that the comparison in Fig. 5 does not involve any adjustable parameter whatsoever, the agree-

ment between simulation and experiment is quite remarkable, and this reiterates our above conclusion that the potential used {Eq. (4)} is accurate enough, and should not be blamed for discrepancies as discussed in connection with Fig. 4.

For the temperatures at which one can equilibrate the system, i.e. here 2750K and higher, it is also possible to determine the self-diffusion constants of Si and O atoms from the simulation. This is done by calculating the mean square displacements  $\langle |\mathbf{r}_i(t) - \mathbf{r}_i(0)|^2 \rangle = \Delta r_\alpha^2(t)$  of the particles of type  $\alpha \in \{\text{Si}, \text{O}\}$ , and apply the Einstein relation  $\Delta_\alpha(t) = 6D_\alpha t$  in the regime of late times where the dependence of  $\Delta_\alpha(t)$  on  $t$  is in fact linear [52,53,54]. The result is shown in Fig. 6, where also the respective experimental data [56,57] are included. As one can see from Fig. 6, one needs to cover 16 decades, from  $10^{-4}\text{cm}^2/\text{s}$  to  $10^{-20}\text{cm}^2/\text{s}$ , to cover the full range including simulation results and experiments, but the simulation results alone are actually restricted to the first four decades of this range only. The straight lines fitted on this Arrhenius plot to the experiment as well as to the simulation show that in this case a bold extrapolation actually is rather successful - but of course there is no guarantee that this will work similarly well in other cases.

A very interesting aspect of the temperature dependence of the diffusion constants is that there are strong deviations from Arrhenius behavior at very high temperatures. It turns out that this region is rather well described by a power law,  $D \propto (T - T_c)^\gamma$ , as it is implied by mode coupling theory, see Eq. (3) with  $D \propto \tau^{-1}$ . In fact, this conclusion is strongly corroborated by a detailed analysis of the intermediate scattering function  $\phi_q(t)$  for wave-vector  $q$  and various other quantities [52]. This finding is somewhat surprising, however, since  $T_c \approx 3330\text{K}$  [52], i.e. far above the melting temperature of crystalline  $\text{SiO}_2$ ! Thus it is no surprise that experimental results had not given hint that mode coupling theory also describes a “strong” glassformer such as  $\text{SiO}_2$  (where  $\tau$  and  $\eta(T)$  follow a simple Arrhenius behavior over a wide range of temperature). Nevertheless, this discovery that a critical temperature exists also for  $\text{SiO}_2$  is of great interest, because it suggests that the differences of the relaxation dynamics between different glassforming fluids are of a quantitative nature only, while qualitatively the behavior is always the same.

### 3 Parallel tempering

One of the major reasons for the slowing down of the dynamics of (atomistic) glass forming systems is that at low temperatures each atom is trapped in a cage formed by its surrounding neighbors. On the other hand the atom itself is part of a cage that trap the neighboring atoms. With decreasing temperature each of these cages becomes stiffer and stiffer and finally each atom can perform only a rattling motion, i.e. the system has become a fluid that doesn’t flow anymore, i.e. a glass. The basic idea of the parallel tempering method is to help the particles to escape their local cage by supplying them with sufficient kinetic energy to overcome the local barrier. Originally proposed for spin models [22,23], the method has been found to be also useful for off-lattice systems. A recent

review on the method can be found in Refs. [24,25]. In the following we discuss briefly how the method is implemented in practice.

If we denote the Hamiltonian of the system as  $H = K(\mathbf{p}) + E(\mathbf{q})$ , where  $K$  and  $E$  are the kinetic and potential energy, respectively, and  $\mathbf{p} = (p_1, p_2, \dots, p_N)$  and  $\mathbf{q} = (q_1, q_2, \dots, q_N)$  are the momenta and coordinates of the particles, we construct a new Hamiltonian  $\mathcal{H}$  as follows:

Make  $M$  independent copies of the Hamiltonian  $H$ :  $H_i = K(\mathbf{p}_i) + E(\mathbf{q}_i)$ . Here the  $\mathbf{p}_i$  and  $\mathbf{q}_i$  are the momenta and coordinates belonging to the  $i$ -th subsystem.  $\mathcal{H}$  is then defined as

$$\mathcal{H}(\mathbf{p}_1, \dots, \mathbf{p}_M, \mathbf{q}_1, \dots, \mathbf{q}_M) = \sum_{i=1}^M H_i(\mathbf{p}_i, \mathbf{q}_i) = \sum_{i=1}^M K(\mathbf{p}_i) + \Lambda_i E(\mathbf{q}_i). \quad (6)$$

The  $1 = \Lambda_1 > \Lambda_2 > \dots > \Lambda_M$  are constants which we will use later. We now make a molecular dynamics simulation of the Hamiltonian  $\mathcal{H}$  at a constant temperature  $T = \beta_0^{-1}$ . After a certain time interval  $\Delta t_{\text{PT}}$  we attempt to exchange the two configurations  $m$  and  $n$  belonging to two neighboring systems (i.e.  $m = n \pm 1$ ). Whether or not the swap of these two configurations is accepted depends on a Metropolis criterion with a acceptance probability

$$w_{m,n} = \begin{cases} 1, & \Delta_{m,n} \leq 0 \\ \exp(-\Delta_{m,n}), & \Delta_{m,n} > 0, \end{cases} \quad (7)$$

where  $\Delta_{m,n} = \beta_0(\Lambda_n - \Lambda_m)(E(\mathbf{q}_m) - E(\mathbf{q}_n))$ . Since the normal molecular dynamics simulation as well as the Monte Carlo procedure on time scale  $\Delta t_{\text{PT}}$  fulfill the condition of detailed balance, the whole algorithm does so also, i.e. after a sufficiently long time the system composed by the subsystem will converge to a Boltzmann distribution. Note that in the systems with a small value of  $\Lambda$  the interaction between the particles is weakened (see Eq. (6)). Therefore it can be expected that the particles in these systems move faster than those in systems with a large value of  $\Lambda$ . Another way to see this is to say that each system is simulated at a different temperature and that periodically the temperature of the system is increased or decreased (hence the name of the algorithm). This walk in temperature space should thus allow the system to overcome the local barriers formed by the above mentioned cages and thus to propagate faster in configuration space.

Note that this algorithm has a substantial number of parameters, all of which influence its efficiency considerably. In order that the acceptance probabilities of Eq. (7) are reasonably high, the coupling constants  $\Lambda_i$  should not be too different. On the other hand one wants that  $\Lambda_M$  is as small as possible since this will lead to a fast propagation of the system at this temperature. Therefore one is forced to choose a relatively large value of  $M$ . This in turn is, however, not good for the overall performance of the algorithm since in order to be ergodic each configuration has to make a random walk in  $\Lambda$ -space, and the time to do this increases like  $M^2$ . Last not least there is the exchange time  $\Delta t_{\text{PT}}$  which should not be too small since then the system just swaps back and forth configurations



that are very similar. On the other hand  $\Delta t_{\text{PT}}$  should also not be too large, since one needs these type of moves in order to explore the  $\Lambda$ -space quickly. The optimal choice of these parameters is currently not known and still the focus of research [58]. A further problem is to find out after which time the system  $\mathcal{H}$  has really equilibrated. It seems that to guarantee this it is not sufficient that every subsystem has visited every point in  $\Lambda$ -space [58,59]. A good random walk should look like the one shown in Fig. 7. Furthermore we point out that it might be possible that a suboptimal choice of these parameters might make the whole algorithm rather inefficient [59].

If the above mentioned parameters of the algorithm are chosen well, the parallel tempering method can indeed speed up the equilibration of the system considerably. This is demonstrated in Fig. 8 where we show the mean squared displacement of the silicon atoms in  $\text{SiO}_2$  as a function of time. From the figure we see that at the lowest temperatures the mean square displacement increases by about a factor of 100 faster than the corresponding curve obtained from the conventional molecular dynamics simulation. From the figure it becomes also clear that the parallel tempering slows *down* the dynamics of the system at high temperatures. This is due to the fact that these systems are coupled to the ones at the low temperatures and hence cannot propagate as fast anymore.

Before we conclude this section we mention that the parallel tempering algorithm has been found to be also very efficient for the equilibration of the Potts glass discussed in the next section. Thus, although the algorithm might have some problems for certain systems or values of parameters, there are models where it seems to work very well.

#### 4 An abstract model for static and dynamic glass transitions: The 10-state mean field Potts glass

In this section we are concerned with a model for which it is known exactly that there is a *dynamical* (ergodic to nonergodic) transition at a temperature  $T_D$  and a second, *static*, transition at a lower temperature  $T_0 < T_D$ , where a static glass order parameter  $q$  appears discontinuously: the infinite range  $p$ -state Potts glass with  $p > 4$  [60,61,62,63,64,65,66]. In this model, one has Potts “spin” variables  $\sigma_i$  which can take one out of  $p$  discrete values which we simply label from 1 to  $p$ ,  $\sigma_i \in \{1, 2, \dots, p\}$ , where  $i$  labels the “sites”,  $i = 1, 2, \dots, N$ . An energy  $pJ_{ij}$  is gained if two spins  $\sigma_i, \sigma_j$  are in the same state,

$$\mathcal{H} = - \sum_{i < j} J_{ij} (p \delta_{\sigma_i \sigma_j} - 1). \quad (8)$$

Every spin interacts with every other spin via an interaction  $J_{ij}$  which is Gaussian distributed, i.e.

$$P(J_{ij}) = \left[ \sqrt{2\pi}(\Delta J) \right]^{-1} \exp\{-(J_{ij} - J_0)^2/[2(\Delta J)^2]\}. \quad (9)$$

Here the mean  $J_0$  and the width  $\Delta J$  are normalized such that

$$J_0 \equiv [J_{ij}]_{av} = \tilde{J}_0/(N-1), \quad (\Delta J)^2 \equiv [J_{ij}^2]_{av} - [J_{ij}]_{av}^2 = \Delta\tilde{J}/(N-1), \quad (10)$$

a choice that ensures a sensible thermodynamic limit. We fix the temperature scale by choosing  $\Delta\tilde{J} \equiv 1$ , and set the mean of the distribution “antiferromagnetic”,  $\tilde{J} = 3 - p$ , in order to avoid any tendency towards ferromagnetic order. (Note that for  $p = 2$  this model would reduce to the standard Ising mean field spin glass (Sherrington-Kirkpatrick model) [67], but we shall be concerned with  $p = 10$  here.) This model, which due to the choice Eq. (9) exhibits quenched random disorder already in the high temperature phase above the glass transition, can be solved exactly in the thermodynamic limit [60,61,62,63,64,65,66]. One finds (Fig. 9) that slightly above  $T_D$  the dynamic auto-correlation function of the spins exhibits a two-step decay, in that a plateau develops whose life-time diverges at  $T_D$ . It is important to note that this behavior is described *exactly* by mode coupling equations of the same type as they occur for the structural glass transition [3]! This shows that this rather abstract model might be more similar to a real structural glass than one would expect at a first glance. At a lower temperature  $T_0$ , a static glass transition occurs [60,61,62,63,64,65,66], where a static order parameter appears discontinuously. Interestingly the static response function does not diverge at  $T_0$ , i.e. the glass susceptibility is still finite here. The entropy does not have a jump at  $T_0$ , but shows only a kink. Thus there is no latent heat associated with this transition! A Kauzmann temperature  $T_K$ , where the (extrapolated) entropy of the high temperature phase would vanish, also exists, but in this case clearly  $T_K < T_0$  and  $T_K$  does not have a physical meaning.

It is of course interesting to know if computer simulations can identify the static and dynamic glass transition in a model for which one knows from the exact solutions [60,61,62,63,64,65,66] that all these glass transitions do indeed exist. Surprisingly, the answer to this question is “no” since very strong finite size effects are present. In particular it is even hard to see that the above mentioned plateau in the autocorrelation function develops as one approaches the temperature  $T_D$  of the dynamical transition (Fig. 10) [28]. This is demonstrated in Fig. 10 where we show the autocorrelation function of the Potts spins as a function of Monte Carlo time, for  $160 \leq N \leq 1280$ . Note that this range is of the same order of magnitude as the particle numbers used for simulations of the structural glass transition, using models such as the binary Lennard-Jones fluid [12] or similar models. No evidence for strong finite size effects was ever found for the latter models if  $N$  was larger than  $\approx 1000$  [68]. Thus, *a priori* it is not at all obvious that system sizes of the order  $10^3$  are completely insufficient to characterize the dynamics of a system in the thermodynamic limit. However, from Fig. 10 we must conclude that for the present system this is indeed the case, at least for temperatures close to the dynamical transition temperature  $T_D$ . This is in contrast with the behavior at a high temperature, e.g.  $T = 1.8$ . From the figure we recognize that at this temperature there are hardly any finite size effects and that the data have nicely converged to the thermodynamic limit even for modest system sizes.

Brangian *et al.* [27,28,29,30] defined a relaxation time  $\tau$  from the time  $t$  that it takes the autocorrelation function to decay to the value  $C(t = \tau) = 0.2$  (broken straight line in Fig. 10). This time is plotted logarithmically versus  $1/T$  in Fig. 11, so an Arrhenius behavior would be a straight line on this plot. One can see rather clearly a crossover from a power law divergence (that would emerge fully in the limit  $N \rightarrow \infty$  for  $T > T_D$ ) to the Arrhenius law at low  $T$ . This behavior qualitatively resembles the behavior expected for structural glasses where the different valleys in the rugged energy landscape for  $T < T_0$  are separated by finite (free) energy barriers. In contrast to this one knows that in the Potts glass in the limit  $N \rightarrow \infty$  these barriers are truly infinite if  $T < T_D$ , and hence the dynamics is strictly nonergodic.

Similar finite size effects affect also the behavior of static properties [27,28,29,30]. One might wonder whether it is possible to use these finite size effects to apply standard finite size scaling analyses to extract reliable information on the location of the static transition temperature from the simulations. Unfortunately the answer is “no”: As figure 12 shows, the standard method [69] of locating a static transition from the intersection point of the order parameter cumulant gives rather misleading results here since the curve seem(!) to intersect at a wrong temperature. Thus one must conclude that there is need to better understand finite size effects for such unconventional glass transitions as sketched in Fig. 9, before one can study them reliably with simulations.

## 5 The bead-spring model: A coarse-grained model for the study of the glass transition of polymer melts

We now draw attention to a model which is intermediate between the abstract model as considered in the previous section and the chemically realistic model of silica melts discussed in Sec. 2. This intermediate model is a coarse-grained model of glassforming polymer melts. Short polymer chains are described by a bead-spring model, with a chain length of  $N = 10$ . The (effective) monomers interact with each other via a truncated and shifted Lennard-Jones potential,

$$U_{LJ}(r) = 4\varepsilon[(\sigma/r)^{12} - (\sigma/r)^6] + C, \quad r \leq r_c = 2.2^{1/6}\sigma \quad (11)$$

while  $U_{LJ}(r) = 0$  if  $r > r_c$ . The constant  $C$  is chosen such that  $U_{LJ}$  is continuous at  $r = r_c$ .

The spring potential present between two neighboring beads is given by

$$U_{\text{FENE}}(l) = -(k/2)R_0^2 \log[1 - (l/R_0)^2] \quad (12)$$

with the following values of the constants [31]:

$$\varepsilon = 1, \sigma = 1, k = 30, R_0 = 1.5. \quad (13)$$

This choice for the parameters creates frustration in the model: the minimum of the bond potential along the chain occurs at a position  $l_{\min} \approx 0.97$  that

is incompatible with the minimum position  $r_{\min} \approx 1.13$  of the Lennard-Jones potential, as far as the formation of simple crystal structures is concerned. This conflict between these two length scales prevents crystallization very efficiently, and the resulting structure of the melt and the corresponding glass resembles corresponding experimental data very nicely, as has already been demonstrated in Fig. 1.

If one carries out “slow” cooling experiments one finds that the volume per monomer shows at a temperature  $T_g \approx 0.41$  a kink [32]. This signals that the system has changed from the liquid branch to the glass branch and hence has fallen out of equilibrium. Qualitatively, the data looks again very similar to that of corresponding experiments [70]. However, if one compares experiment and simulation more quantitatively, one notes again a big disparity in the cooling rates: In the simulation the temperature was reduced by  $\Delta T = 0.02$  every 500000 MD time steps, each time step being  $\delta t = 0.002\tau_{MD}$  with  $\tau_{MD} = \sigma(m/\varepsilon)^{1/2}$ ,  $m$  being the effective mass of the monomeric units. If one estimates that  $\tau_{MD}$  corresponds roughly to  $10^{-11}$ s, and that  $T = 1$  corresponds to 500K, one arrives at a cooling rate of  $\Delta T/\Delta t \approx 10^9$ K/s. While this estimate is three orders of magnitude smaller than the corresponding cooling rate for the silica melts [50], it is still many orders of magnitude larger than the corresponding experimental cooling rates. Hence also in this case there is a huge gap between the cooling rates accessible in simulations and those used in real experiments.

This model yields also qualitatively very reasonable results for the relaxation dynamics: The self-diffusion constant can be fitted well by the Vogel-Fulcher law given by Eq. (1), with  $T_{VF} \approx 0.34$ , below the kink temperature  $T_g \approx 0.41$ . The mode coupling critical temperature is located at  $T_c \approx 0.45$ , above the kink temperature, and the ratios  $T_c/T_g$  and  $T_c/T_{VF}$  are quite reasonable. Although in the simulation only 1200 monomers were used, a nice plateau is found in the intermediate incoherent scattering function  $\phi_q^s(t)$ , see Fig. 13. Hence one can conclude that no strong finite size effects are present for this model.

Also the Rouse modes [71] which describe the mesoscopic Brownian motion of the polymer chains on length scales that are between monomer-monomer distances and the coil size, are found to relax over almost two decades in  $T - T_c$  with relaxation times that show the mode coupling power law [33], see Fig. 14. Only very close to  $T_c$ , for  $T \leq 0.46$ , can one see small indications that the singularity at  $T_c$  is in fact rounded off. This model has allowed many very impressive tests [35,37] of mode coupling theory, similar to an often studied binary Lennard-Jones mixture [12,72]. But similar to the case in the latter model, it has so far turned out impossible to study temperatures for  $T < T_c$  in thermal equilibrium. And none of these models - neither the model for  $\text{SiO}_2$ , nor the binary Lennard-Jones model [12] nor the present beadspring model - could provide any clarification about the validity of the entropy theory [17].

## 6 The bond fluctuation model approach to glassforming polymer melts

The bond fluctuation model [6,38,39,40,41,42,43,44,45,46,47] is an even more abstract model of polymers than the bead-spring model discussed in the previous section, since it forces the chains to “live” on a simple cubic lattice, and all motions on scales smaller than a lattice constant are completely suppressed. In this model a polymer is represented again as a chain of effective monomers connected by effective bonds, but now each effective monomer is described by an elementary cube on the lattice that blocks all 8 sites at the corners of the cube from further occupation (Fig. 15). The length of the effective bonds is allowed to vary from 2 to  $\sqrt{10}$  lattice constants (taken as length unit in this section). The only nonbonded interaction is the one of excluded volume. The dynamics of the random conformational changes of the real polymer is represented in a crude way by attempted hops of randomly chosen monomers in randomly chosen lattice directions. If about one half of all lattice sites are occupied, the system behaves like a dense melt, and even short chains with chain length  $N = 10$  show already typical polymer-properties, e.g. the scaling of the radius of gyration with  $\sqrt{N}$ , etc.

Since real polymers show with decreasing temperature an increase of the persistence length and hence of the chain radius, it is natural to model this effect by an effective potential  $U(l)$  for the length of the effective bonds, energetically favoring long bonds. If one chooses as a minimum of this potential  $U(l_{\min} = 3) = 0$  while  $U(l) = \varepsilon = 1$  for all other bond lengths  $l$ , one also incorporates “geometric frustration” (Fig. 15) into the model: Each bond that reaches its ground state wastes the four lattice sites in between the adjoining effective monomers, which are completely blocked for further occupation. From the point of view of packing as many effective monomers as possible in a dense melt on the lattice, the bonds that waste lattice sites are very unfavorable. Hence configurational entropy favors short bonds that do not waste any other lattice sites for further occupation. Thus a conflict between entropy and energy is created, which is responsible for the glass transition observed in the Monte Carlo simulations of this model.

This model has the big technical advantage that it can be equilibrated even at relatively low temperatures by the so-called “slithering snake algorithm”. In this type of Monte Carlo moves one randomly attempts to remove a bond from one chain end and attach it to the other chain end in a randomly chosen orientation [44]. Although this algorithm does not correspond to any physically realistic dynamics of polymers it is a perfectly admissible Monte Carlo move for studying equilibrium properties. Using this algorithm, thermal equilibrium can be established at rather low temperatures, such as  $T = 0.16$ , where after  $10^7$  steps with the conventional “random hopping” algorithm the autocorrelation of the end-to-end vector of the chains still has not decayed below 90% of its starting value [46]. If we wish to study dynamical properties of this model, we first perform a run with this slithering snake algorithm, to obtain initial states that are characteristic for thermal equilibrium. Subsequently we can start a run with the normal random hopping moves of the effective monomers, which thus

yields a physically reasonable description of the dynamics [46]. If one estimates that one Monte Carlo Step per monomer corresponds to about  $10^{-12}$  seconds in real time, a run of  $10^7$  steps would reach a physical time of  $10^{-5}$  seconds, which is several orders of magnitude longer than the typical time scales accessible with molecular dynamics. Using this algorithm it was hence possible to make a very nice test of mode coupling theory [42,43], resulting in  $T_c \approx 0.15$  while [46]  $T_{VF} = 0.125 \pm 0.005$ . However, the investigation of the relaxation dynamics in the regime  $T_{VF} < T \leq T_c$  seems to be very difficult also in the framework of this lattice model, and in fact has not yet been attempted.

Using the bond fluctuation model it was also determined how the glass transition temperature  $T_g$  depends on the length of the chain [41] and the results are compatible with the law

$$T_g(\infty) - T_g(N) \propto 1/N. \quad (14)$$

Such a dependence has also been found experimentally [73], and is one of the most notable predictions of the entropy theory of Gibbs and Di Marzio [17]. Therefore many experimentalists believe that this theory is correct. However, this conclusion is premature, as a study of the configurational entropy for the present lattice model shows (Fig. 16). While the entropy does indeed decrease rather strongly with increasing value of inverse temperature, starting out from an “athermal melt” (corresponding to infinite temperature), this decrease becomes slower when one approaches the vicinity of  $T_c$ , and the simulation data do not show that the entropy vanishes, although they also cannot rule it out that this happens at a  $T$  far below  $T_c$ . However, if one works out the Gibbs-Di Marzio theory [17] explicitly for the present lattice model (all the input parameters of the theory [17] can also be extracted from the simulation, so there are no adjustable parameters whatsoever in this comparison!), one sees that the theory underestimates the actual entropy considerably at all temperatures. In particular this failure is responsible for the vanishing of the entropy at  $T_K \approx 0.18$ , which obviously is a spurious result, since this temperature is even higher than  $T_c$ , well in the melt regime where the polymer system is a liquid and not a glass. In fact, a slightly different approximation due to Milchev [75] renders the entropy nonnegative at all temperatures, but deviates now a bit from the simulation data in the other direction. Thus, these investigations show that although Eq. (14) does indeed hold it does not imply anything about the validity of the Kauzmann “entropy catastrophe”.

## 7 Can one map coarse-grained models onto atomistically realistic ones?

From the above comments it is clear that in simulations of simplified coarse-grained models the range of times one can span is much larger than the one for chemically realistic models that include atomistic detail (microseconds rather than nanoseconds). On the other hand, the simplified models may elucidate

general concepts but they fail to make quantitative predictions on the properties of particular materials. Thus the question arises whether one can somehow combine the advantages of both approaches.

An idea to do this is to make the coarse-graining process in a more systematic way and to construct coarse-grained models that “remember” from which atomistic system they come from. For a polymer chain, coarse-graining along the backbone of the chain may mean that if we label the covalent bond consecutively (1, 2, 3, 4, 5, 6, ...) the bonds 1, 2, 3 form the effective bond  $I$ , the bonds 4, 5, 6 form the effective bond  $II$ , etc [76]. The potentials on the atomistic scale (e.g. potentials controlling the lengths of covalent bonds, the angles between them, the torsional angles, etc.) have then to be translated into suitable effective potentials for the length  $l$  of the effective bonds and the angle  $\Theta$  between them. The simplest choice would be to assume potentials of the form

$$U_{\text{eff}}(l) = \frac{1}{2}u_0(l - l_0)^2, V_{\text{eff}}(\Theta) = \frac{1}{2}v_0(\cos \Theta - \cos \Theta_0)^2 \quad . \quad (15)$$

In the past potentials of this type have indeed been extracted from the probability distributions  $P(l) \propto \exp[-U_{\text{eff}}(l)/k_B T]$ ,  $P(\Theta) \propto \exp[-V_{\text{eff}}(\Theta)/k_B T]$  observed in the simulations of single chains (where long range interactions need to be truncated, however) [76,77]. Of course, the effective parameters  $u_0, l_0, v_0, \Theta_0$  are somewhat temperature dependent, and in principle one should deduce them from simulations of atomistically described melts containing many chains, rather than from single-chain simulations [77]. The practical implementation of how one constructs best the effective potentials that mimic one particular material is still an active topic of research [48,77].

A further important aspect is the question to what extent the dynamics with such a coarse grained system reflects the dynamics of a real chain. Here one needs to focus on the slowest local process, which are hops of small groups of monomers to a new conformation, such that a barrier of the torsional potential is crossed. Without such moves involving barrier crossing no conformational changes can occur. In a typical case, e. g. for polyethylene at  $T = 500\text{K}$ , the time scale for such hops is about two orders of magnitude larger than the vibration times of bond lengths and bond angles. Only because of this separation of time scales one can hope that a coarse-grained model can describe the essential features of the slow dynamics in the polymer melt at all, if the time units are properly rescaled. As shown by Tries *et al.* [48], the knowledge of the torsional potentials allows, using an approach that resembles transition state theory, to construct a “time rescaling factor”, that gives the translation of the time unit of the Monte Carlo simulations (attempted Monte Carlo steps per monomer) into physical time units (Fig. 17). One sees that for polyethylene 1 Monte Carlo step corresponds to 0.1 to 10ps, in the temperature region of interest. At high temperatures, namely for  $T = 509\text{K}$ , the accuracy of the coarse-grained model of  $\text{C}_{100}\text{H}_{202}$  was tested by running a molecular dynamics simulation of a united atom model for about a nanosecond (which is of the order of the Rouse relaxation time at this temperature) for comparison [48]. It is found that the agreement between both approaches is almost quantitative. The advantage of the Monte Carlo simulation of the coarse-

grained model is, however, that one can easily study a supercooled melt also at  $T = 250\text{K}$ , a temperature which is basically inaccessible to the molecular dynamics approach.

If one compares the results of the coarse-grained model to experimental data, e. g. for the viscosity and its temperature dependence, the agreement is encouragingly good but not perfect [48]. One aspect which is clearly missing in the coarse-grained model is the description of attractive intermolecular forces. Thus, while this approach of mapping atomistic models to coarse-grained ones clearly has a great potential, there are still nontrivial problems that need to be solved.

## 8 Concluding remarks

In this brief review, the “state of the art” of computer simulations of glassy systems was summarized. The main problem in this field is the problem of bridging time scales - a supercooled fluid close to the glass transitions exhibits a nontrivial dynamic behavior that extends from very fast processes (in the picosecond time scale range) to very slow processes (with relaxation times of the order of hours). Atomistic molecular dynamics simulations of chemically realistic models (as exemplified here for the case of molten  $\text{SiO}_2$ ) can treat only a very small part of this broad range of time scales, and also special techniques such as the parallel tempering method can add only one or two decades to this range but not more. (Note also that there are still some unsolved technical problems with this method [59]). While such atomistic simulations are nevertheless useful, in particular since they complement the time range directly accessible to experiment, and give a very detailed insight into the interplay between structure and dynamics in supercooled fluids, they clearly cannot answer questions on the nature of relaxation processes for temperatures close to (the experimental)  $T_g$ , and the possible existence for an underlying static phase transition (from a metastable supercooled fluid to a metastable ideal glass) at a temperature  $T_K < T_g$ . Also molecular dynamics studies of coarse-grained models for melts of short, unentangled polymer chains suffer from similar problems, although the effective cooling rates in these models are about a factor of  $10^3$  smaller than in the model for silica, and one can access relaxation times that are almost in the microsecond range. These models are very useful as a testbed for the mode coupling description of the glass transition in fragile glassformers, however. Furthermore they have also allowed to gain very useful insight on the relaxation between the local motions responsible for the glass transition (cage effect etc.) and the more mesoscopic Brownian motion of the polymer chains (as described by the “Rouse modes”, for instance).

A slightly more abstract model of the same systems, the bond fluctuation model of glassforming polymer melts, corroborates these conclusions, although due to its discrete nature it is somewhat less suitable to describe the local structure of packing effective monomers in a polymer melt or their motion on small scales (confined in a cage). However, this model has the merit that it allows to compute the temperature dependence of the configurational entropy  $S(T)$  and



thus to test the correctness of theories like the one of Gibbs and Di Marzio. While it is found that the entropy  $S(T)$  decreases significantly if the polymer melt approaches the glass transition, there is clear evidence that the theory of Gibbs and Di Marzio is quantitatively very unreliable since it underestimates  $S(T)$  significantly at all temperatures, and the “entropy catastrophe” that it predicts is clearly an artifact of inaccurate approximations.

Finally, studies of an even more abstract model were discussed, the 10-state Potts glass with mean field infinite range interactions. This model has the advantage that it is known exactly that it has a dynamical (ergodic to nonergodic) transition at  $T_D$  as well as a static transition at a (slightly) lower temperature  $T_0$ , at which a glass order parameter appears discontinuously and the entropy shows a kink. The conceptual disadvantage of this model, however, is that it has a built-in quenched random disorder (via its random exchange couplings) at all temperatures, unlike systems that undergo a structural glass transition, which have no quenched disorder in the high temperature phase (the supercooled fluid for  $T > T_g$ ). Monte Carlo studies of this model, intended to serve as a general testbed for systems with both a dynamical and a static glass transition, show that unexpectedly large finite size effects occur, which are poorly understood. Thus even for this “simple” model much more work is necessary.

While the anticipated progress in computer hardware and algorithmic improvements will allow to extend the time ranges accessible in all these simulations somewhat, there is not real hope that one can bridge the desired 15 (or more) decades in time in this way. More promising in principle is the approach of providing an explicit mapping between atomistic models (which cover the fast processes) and coarse-grained models (which describe the somewhat slower processes, in the 10ps to 1 $\mu$ s range), so that one effectively considers the same model system but with different approaches on different time scales. Of course, this idea is difficult to work out consistently in practice, and only modest first steps towards its realization have been taken. Much more work in this direction is certainly very desirable in the future.

**Acknowledgements:** We are particularly grateful to C. Bennemann, C. Brangian, J. Horbach, T. Stühn, K. Vollmayr, and M. Wolfgardt for their valuable collaboration on parts of the research described here, and acknowledge financial support from the Deutsche Forschungsgemeinschaft (DFG/SFB 262), the Bundesministerium für Bildung und Forschung (BMBF grant No 03N6015) and SCHOTT Glas. We thank the NIC Jülich and the HLRS Stuttgart for generous allocations of computer time.

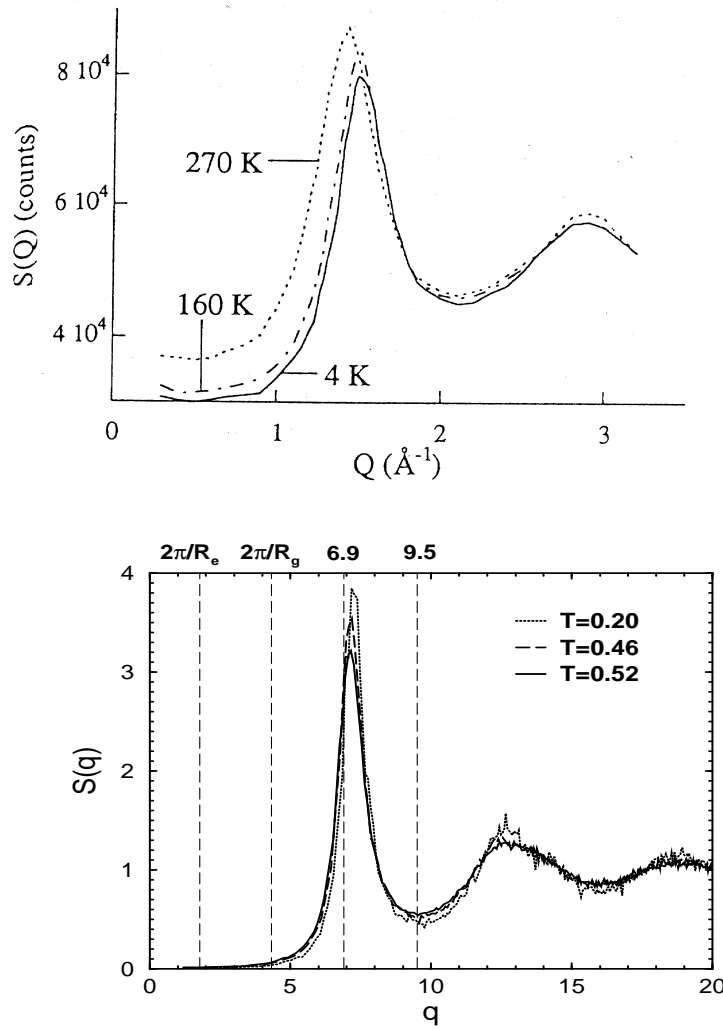


**Fig. 1.** a) Static collective structure factor of polybutadiene at temperatures  $T = 4\text{K}$ ,  $T = 16\text{K}$ , and  $T = 270\text{K}$ . Note that for this system the glass transition temperature is  $T_g = 180\text{K}$  and the critical temperature of mode coupling theory [3] is  $T_c = 220\text{K}$ . The scattering background is not subtracted here, thus the zero of the ordinate axis is not known precisely, and the ordinate units are just measuring absolute scattering intensities. From Arbe *et al.* [13]. b) Static collective structure factor  $S(q)$  plotted versus wave-vector  $q$ , for a bead-spring model of flexible polymer chains with chain length  $N = 10$ . Beads interact with the potential given in Eqs. (11)-(13), and lengths are measured in units of  $\sigma$ , temperatures in units of  $\varepsilon$ . Three temperatures  $T = 0.2$ ,  $0.46$  and  $0.52$  are shown (note that  $T_g \approx 0.41$  and  $T_c \approx 0.45$  for this model). The vertical lines highlight characteristic inverse length scales (related to the end-to-end distance  $R_e$  and radius of gyration  $R_g$  of the chains as well as the first maximum and minimum of  $S(q)$ ). From Baschnagel *et al.* [14].

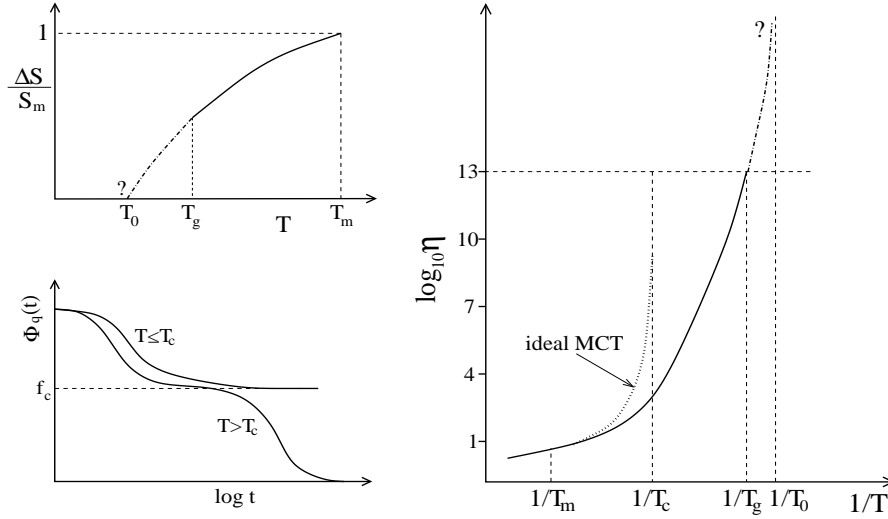


**Fig. 2.** Right figure: Schematic plot of the viscosity  $\eta(T)$  of a fluid (note  $\eta(T) \propto \tau$ ) vs. inverse temperature  $1/T$ . The location of the melting temperature ( $T_m$ ), the critical temperature of mode coupling theory ( $T_c$ ) [3], the glass transition temperature ( $T_g$ ) and the Vogel-Fulcher-Kauzmann temperature [1,15] ( $T_0$ ) are shown on the abscissa. The glass transition temperature  $T_g$  is defined empirically requiring [1]  $\eta(T = T_g) = 10^{13}$  Poise. Two complementary concepts to explain the glass transition are indicated by the schematic plots on the left: The lower figure shows the time correlation function  $\Phi_q(t)$  for density fluctuations at wave-vector  $q$  which according to idealized mode coupling theory shows at a temperature  $T_c$  a nonzero “non-ergodicity parameter”  $f_c$  [3]. For  $T$  somewhat larger than  $T_c$ ,  $\Phi_q(t)$  exhibits a plateau and the “lifetime”  $\tau$  of this plateau (as well as  $\eta$ ) diverge as one approaches  $T_c$  [3]. The upper figure shows the entropy difference  $\Delta S(T) = S_{\text{fluid}} - S_{\text{crystal}}$ , with  $S_m \equiv \Delta S(T_m)$ . The linear extrapolation of  $\Delta S$  for  $T < T_g$  defines the Kauzmann temperature  $T_0$  via  $\Delta S(T = T_0) = 0$  [15]. Adapted from Binder [16].

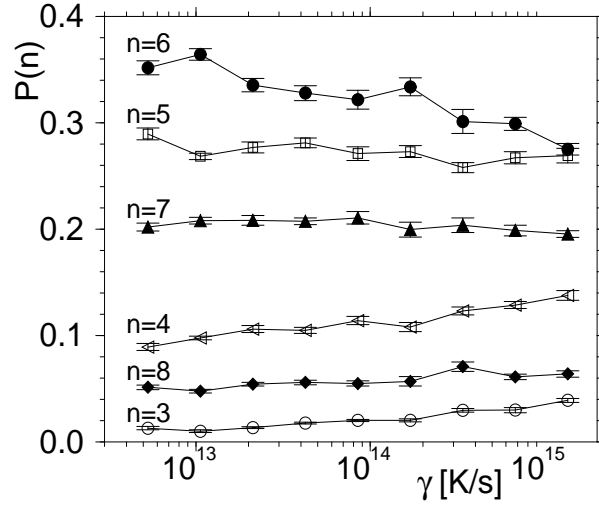


**Fig. 3.** Cooling rate dependence of the probability  $P(n)$  that in the network structure of  $\text{SiO}_2$  a ring of size  $n$  is present. A ring is defined as the shortest connection of consecutive Si-O elements that form a closed loop and  $n$  is the number of these segments. In this simulation we used 668 oxygen and 334 Si-atoms, and cooled the sample at constant pressure  $p = 0$  in an  $NpT$  simulation, cooling from the initial temperature  $T_i = 7000\text{K}$  to the final temperature  $T = 0\text{K}$ . An average over 10 independent runs was performed, allowing to estimate the statistical errors given in the figure. From Vollmayr *et al.* [50].

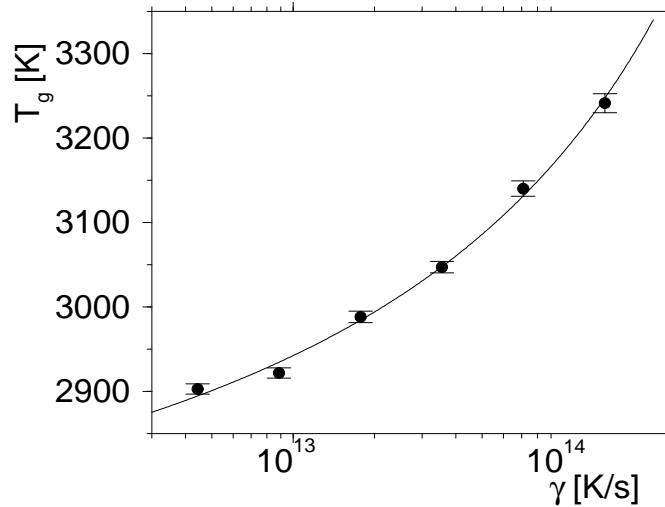


**Fig. 4.** Effective glass transition temperature  $T_g(\gamma)$  plotted vs. the cooling rate  $\gamma$ , for molecular dynamics simulations of  $\text{SiO}_2$  using the BKS potential [49] and estimating  $T_g(\gamma)$  from intersection points of fit functions to the enthalpy, as described in the text. All data are based on averages over 10 statistically independent runs. The curve is a fit to the function given in Eq. (5) of the text, resulting in  $T_{VF} = 2525\text{K}$ . From Vollmayr *et al.* [50].

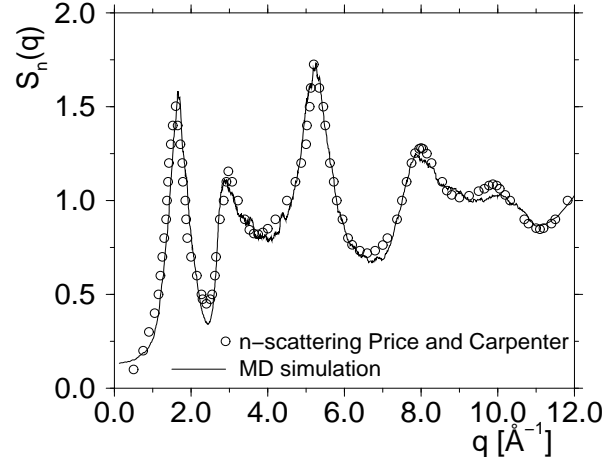


**Fig. 5.** Static neutron structure factor of  $\text{SiO}_2$  at room temperature ( $T = 300\text{K}$ ) plotted versus wave-vector  $q$ . The full curve is the molecular dynamics simulation of Ref. [52], using the experimental neutron scattering lengths for Si and O atoms, while the symbols are the neutron scattering data of Ref. [55]. From Horbach and Kob [52].

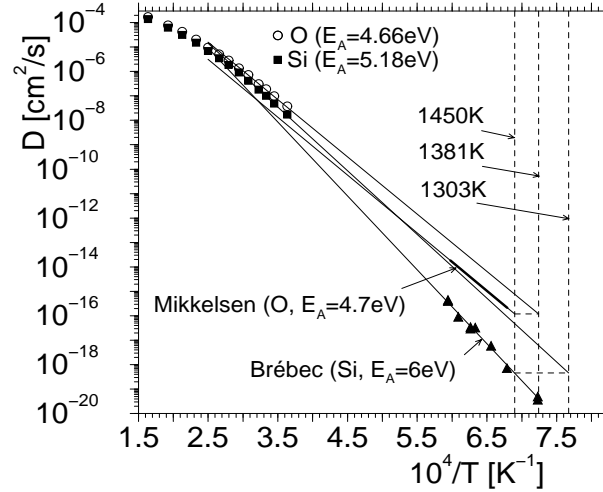


**Fig. 6.** Plot of the self-diffusion constant  $D$  of silicon atoms (Si) and oxygen atoms (O) in molten  $\text{SiO}_2$  as a function of inverse temperature. The symbols in the upper left part are the results from molecular dynamics simulations and the data in the lower right part stems from experiments [56,57]. The thin straight lines show simple Arrhenius behavior  $\{D \propto \exp(-E_A/k_B T)\}$  with various choices of the activation energy  $E_A$ , as indicated in the figure. The vertical broken lines indicate the experimental glass transition temperature,  $T_g = 1450\text{K}$ , as well as values for  $T_g$  that one obtains if one extrapolates the data from the simulations to low temperatures and then estimates  $T_g$  from the experimental value of the O diffusion constant  $\{D_{\text{O}}(T = T_g^{\text{sim}}) = 10^{-16}\text{cm}^2/\text{s} \Rightarrow T_g^{\text{sim}} = 1381\text{K}$  or the Si diffusion constant, respectively  $\{D_{\text{Si}}(T = T_g^{\text{sim}}) = 5 \cdot 10^{-19}\text{cm}^2/\text{s} \Rightarrow T_g^{\text{sim}} = 1303\text{K}$ . From Horbach and Kob [52].

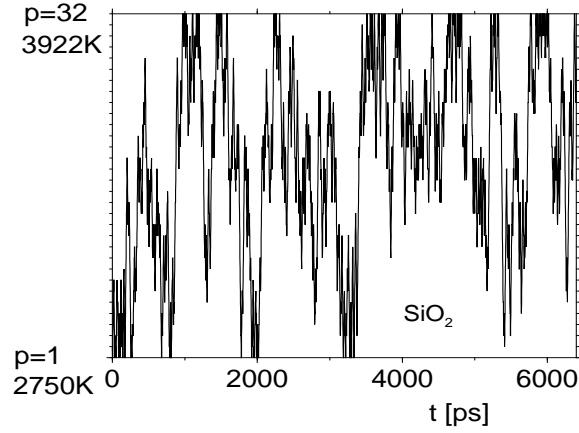


**Fig. 7.** Time dependence of the coupling constant for a parallel tempering simulation of liquid  $\text{SiO}_2$ . The number of particles was 336 and the number of subsystems was 32. Note that the shown subsystem visits all the different coupling constants several times, thus giving evidence that the overall system has indeed reached equilibrium. From Kob *et al.* [26].

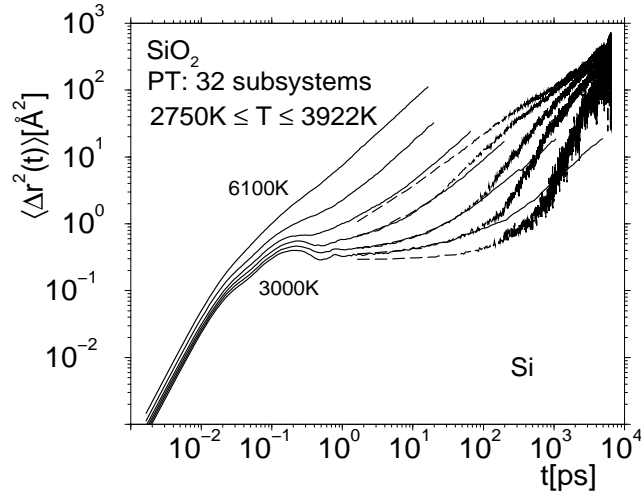


**Fig. 8.** Time dependence of the mean squared displacement of Si in  $\text{SiO}_2$  at different temperatures. The dashed lines are from parallel tempering runs and correspond to temperatures 3922K, 3585K, 3235K, 3019K, and 2750K (top to bottom). The solid lines are from conventional molecular dynamics runs and correspond to temperatures 6100K, 4700K, 4000K, 3580K, 3250K, and 3000K (top to bottom). From Kob *et al.* [26].

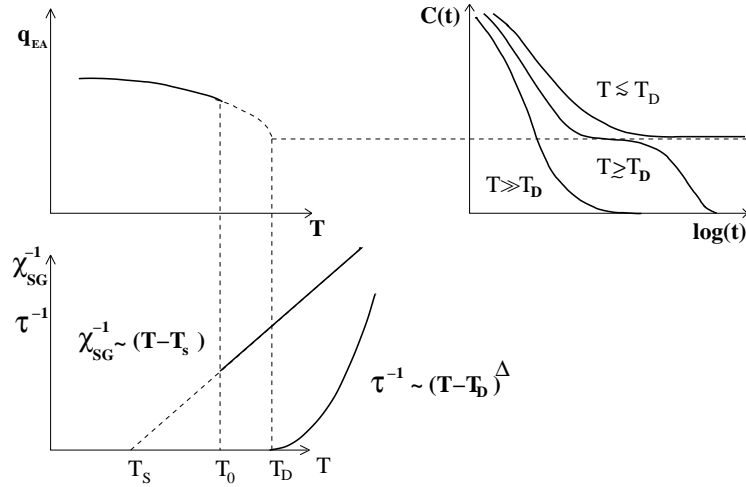


**Fig. 9.** Mean-field predictions for the  $p$ -state Potts glass with  $p > 4$ . The spin glass order parameter,  $q_{EA}$ , is nonzero only for  $T < T_0$  and jumps to zero discontinuously at  $T = T_0$ . The spin glass susceptibility  $\chi_{SG}$  follows a Curie-Weiss-type relation with an apparent divergence at  $T_S < T_0$ . The relaxation time  $\tau$  diverges already at the dynamical transition temperature  $T_D$ . This divergence is due to the occurrence of a long-lived plateau of height  $q_{EA}$  in the time-dependent spin autocorrelation function  $C(t)$ . The discontinuous transition of the order parameter, however, is not accompanied by a latent heat. Therefore, there is no jump in the entropy at  $T_0$ , but only a kink occurs. The extrapolation of the high-temperature branch of the entropy would vanish at a “Kauzmann temperature”  $T_K = [(1/4)(p-1)/\ln p]^{1/2}T_S \approx 0.988T_S$ . From Brangian *et al.* [30].

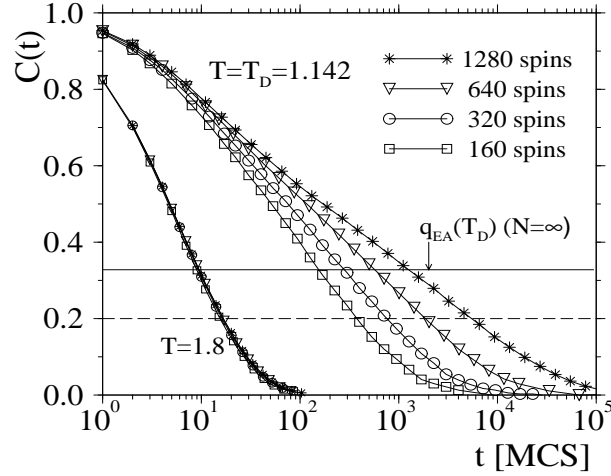


**Fig. 10.** Time dependence of the autocorrelation function  $C(t)$  of the spins in the 10-state mean field Potts glass.  $C(t)$  is normalized such that  $C(t = 0) = 1$  and  $C(t \rightarrow \infty) = 0$  for  $T > T_D$ . Time is measured in units of Monte Carlo steps per spin [MCS]. Two temperatures are shown,  $T = 1.8$  and  $T = T_D = 1.142$  [66], for several values of  $N$ . The solid horizontal line indicates the theoretical value of the Edwards-Anderson order parameter  $q_{EA}(T_D) \equiv C(t \rightarrow \infty)$  at  $T \rightarrow T_D^-$  for  $N \rightarrow \infty$  [66]. The horizontal dashed line shows the value used to define the relaxation time  $\tau$ ,  $C(t \equiv \tau) = 0.2$ . From Brangian *et al.* [28].

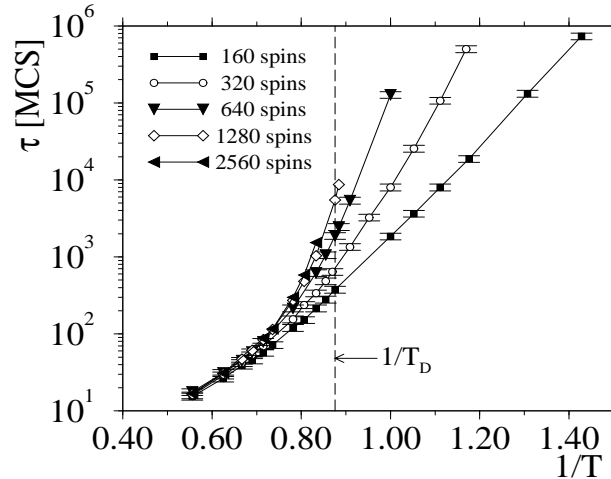


**Fig. 11.** Arrhenius plot of the relaxation time  $\tau$  of the 10-state mean field Potts glass model for different system sizes. Error bars of  $\tau$  are mostly due to sample-to-sample fluctuations. The vertical dashed line is the location of  $T_D$  where, for  $N \rightarrow \infty$ , the relaxation time is predicted to diverge with a power-law. From Brangian *et al.* [28].



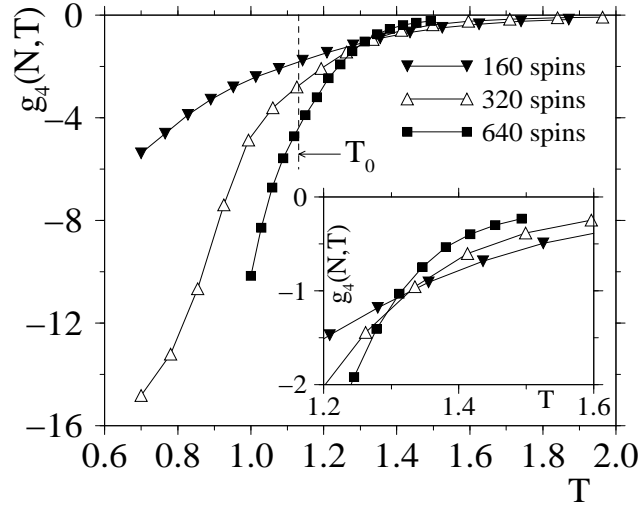


**Fig. 12.** Temperature dependence of the order parameter cumulant  $g_4(N, T) = \frac{(p-1)^2}{2} \left\{ 1 + \frac{2}{(p-1)^2} - \frac{[(q^4)_{av}]}{[(q^2)_{av}]} \right\}$  for the 10-state mean field Potts glass for three choices of  $N$  ( $N = 160, 320$  and  $640$ ). (Here  $q$  is the order parameter.) The vertical straight line shows the location of the static transition temperature  $T_0$  as predicted by the exact solution [66]. The inset is an enlargement of the region where the three curves intersect. From Brangian *et al.* [28].

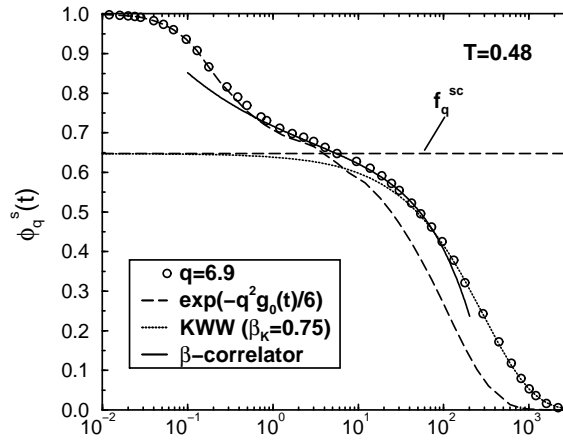


**Fig. 13.** Comparison of the incoherent intermediate scattering function  $\phi_q^s(t)$  for the bead-spring model at  $T = 0.48$  and  $q \approx 6.9$  [ $\approx$  maximum of  $S(q)$ , cf. Fig. 1] with various approximations: a Gaussian approximation (dashed line),  $\phi_q^s = \exp[-q^2 g_0(t)/6]$ , where  $g_0(t)$  is the mean square displacement of the monomers. The mode coupling fit for the regime of the so-called “ $\beta$ -relaxation” (solid-line) and a fit with the Kohlrausch function {Eq. (2), dotted line} also are included. The non-ergodicity parameter  $f$  is indicated as a horizontal dashed line. From Baschnagel *et al.* [14].

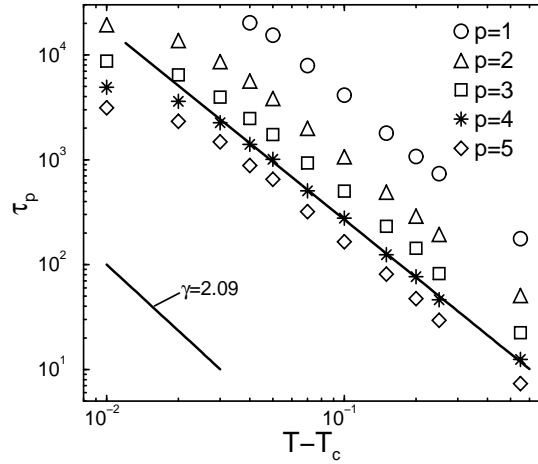


**Fig. 14.** Variation of the relaxation time  $\tau_p$  of the Rouse modes with the mode index  $p$  for the bead spring model plotted vs.  $T - T_c$ , showing also a power law fit for  $p = 4$  ( $\gamma_p = 1.83 \pm 0.02$ ). Within the error bars, this slope provides a reasonable fit for all  $p$  shown. From Baschnagel *et al.* [33].

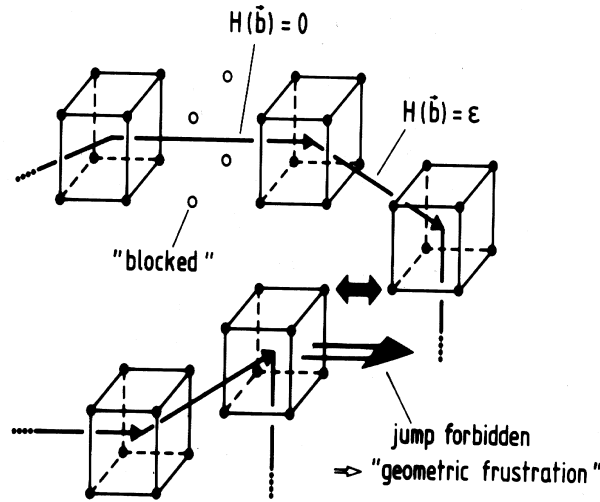


**Fig. 15.** Sketch of a possible configuration of monomers belonging to two different chains in the bond fluctuation model of a polymer melt. For one monomer of the lower chain, an attempted move is indicated; this jump is forbidden, however, since it violates the excluded volume constraint. Also the choice of a two-state energy function is indicated, namely  $\mathcal{H}(\vec{b}) = 0$  if the bondvector  $\vec{b}$  equals  $\vec{b}_{\min} = (0, 0, \pm 3a)$  or a permutation thereof ( $a$  is the lattice spacing, chosen as unit of length in the following), and  $\mathcal{H}(\vec{b}) = \epsilon = 1$  else. Note that if a bond takes a ground state bond  $\vec{b}_{\min}$  it blocks automatically 4 sites (the 4 sites are highlighted by empty circles). From Baschnagel *et al.* [39].

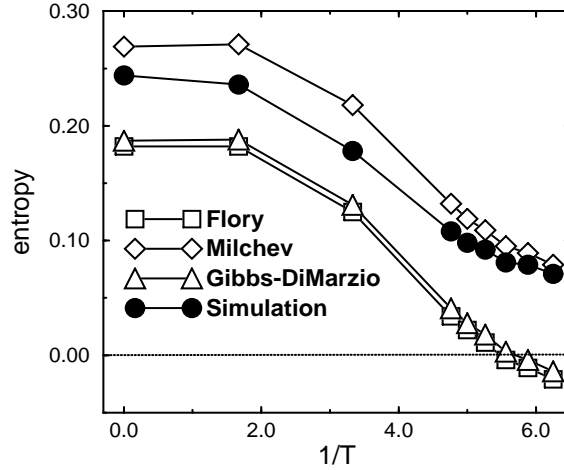


**Fig. 16.** Comparison of the temperature dependence of the entropy per lattice site as obtained from the simulation of the bond fluctuation model (open circles) with the theoretical predictions of Gibbs and Di Marzio [17], Flory [74] and Milchev [75]. Note that the estimates for  $T_c$  and  $T_{VF}$  are  $T_c \approx 0.15$  and  $T_{VF} \approx 0.125$ . Therefore the vanishing of the entropy at  $T \approx 0.18$  is an artifact due to inaccurate approximations involved in the calculation of  $S(T)$  via the entropy theory [17]. From Wolfgardt *et al.* [45].

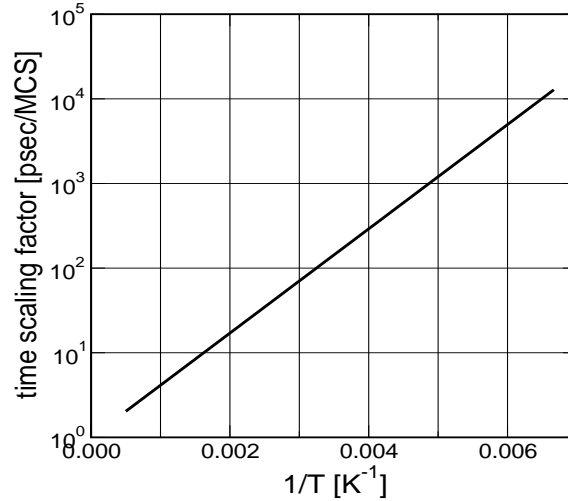


**Fig. 17.** Temperature dependence of the time scaling factor converting the time unit of the Monte Carlo simulation into femtoseconds, for the case of polyethylene. The straight line shows that a simple Arrhenius law is a good approximation. Adapted from Ref. [48].

## References

1. J. Jäckle: Rep. Progr. Phys. **49**, 171 (1986)
2. K. L. Ngai (Ed.): *Proceedings of the First International Meeting on Relaxations in Complex Systems*, J. Non-Cryst. Solids **131-133** (1991)
3. W. Götze, J. Sjögren: Rep. Progr. Phys. **55**, 214 (1992)
4. K. L. Ngai (Ed.): *Proceedings of the Second International Discussion Meeting on Relaxations in Complex Systems*, J. Non-Cryst. Solids **172-174** (1994)
5. K. L. Ngai (Ed.): *Proceedings of the Third International Discussion Meeting on Relaxations in Complex Systems*, Non-Cryst. Solids **235-237** (1998)
6. W. Paul, J. Baschnagel: "Monte Carlo simulation of the glass transition of polymers". In: *Monte Carlo and Molecular Dynamics Simulations in Polymer Science* ed. by K. Binder (Oxford University Press, New York 1995) pp. 307-355.
7. K. Binder, W. Kob: "How can computer simulations contribute to understand the static structure of glasses". In: *Analysis of the Composition and Structure of Glass and Glass Ceramics* ed. by H. Bach and D. Krause (Springer, Berlin 1999) pp. 255-267
8. W. Kob, K. Binder: "How can computer simulations contribute to the understanding of the dynamics of glasses and glass melts?" In: *Analysis of the Composition and Structure of Glass and Glass Ceramics* ed. H. Bach and D. Krause (Springer, Berlin 1999) pp. 344-356.
9. K. Binder: Computer Phys. Commun. **121-122**, 168 (1999)
10. K. Binder: J. Non-Cryst. Solids **274**, 332 (2000)
11. K. Binder, J. Baschnagel, W. Paul: Progr. Polymer Sci. (in press)
12. W. Kob: J. Phys.: Cond. Matter **11**, R85 (1999)
13. A. Arbe, D. Richter, J. Colmenero, B. Farago: Phys. Rev. E **54**, 3853 (1996)
14. J. Baschnagel, C. Bennemann, W. Paul, K. Binder: J. Phys.: Condens. Matter **12**, 6365 (2000)
15. W. Kauzmann: Chem. Rev. **43**, 219 (1948)
16. K. Binder: Ber. Bunsenges. Phys. Chem. **100**, 1381 (1996)
17. J. H. Gibbs, E. A. Di Marzio: J. Chem. Phys. **28**, 373 (1958)
18. G. Adam, J. H. Gibbs: J. Chem. Phys. **43**, 739 (1965)
19. M. Fuchs, W. Götze, S. Hildebrand, A. Latz: J. Phys.: Condens. Matter **4**, 7709 (1992)
20. M. P. Allen, D. J. Tildesley: *Computer Simulation of Liquids* (Clarendon Press, Oxford, 1987)
21. K. Binder, G. Ciccotti (eds.): *Monte Carlo and Molecular Dynamics of Condensed Matter Systems* (Societa Italiana di Fisica, Bologna, 1996)
22. E. Marinari and G. Parisi, Europhys. Lett. **19**, 451 (1992)
23. K. Hukushima, K. Nemoto: J. Phys. Soc. Jpn. **65**, 1604 (1996)
24. U. H. E. Hansmann and Y. Okamoto, Annual Rev. of Comp. Phys. Vol. VI, (World Scientific, Singapore, 1999) p. 179
25. Y. Iba, Int. J. Mod. Phys. C **12** 623 (2001)
26. W. Kob, C. Brangian, T. Stühn, R. Yamamoto: "Equilibrating Glassy Systems with Parallel Tempering" In: *Computer Simulation Studies in Condensed Matter Physics XIII* ed. by D. P. Landau, S. P. Lewis, H. P. Schüttler (Springer, Berlin, 2001) pp. 153-166.
27. C. Brangian, W. Kob, K. Binder: Europhys. Lett. **53**, 756 (2001)
28. C. Brangian, W. Kob, K. Binder: J. Phys. A: Math. Gen. (in press)

29. C. Brangian, W. Kob, K. Binder: "Static and dynamics glass transitions in the 10-state Potts glass: What can Monte Carlo simulations contribute?" In: *Proceedings of the STATPHYS 21 Satellite meeting: Computational Statistical Mechanics - Challenges for the 21<sup>st</sup> Century* ed. by D. P. Landau (in press)
30. C. Brangian, W. Kob, K. Binder: "Monte Carlo study of the dynamic and static glass transition in the 10-state Potts glass: A scenario for the structural glass transition?" In: H. E. Stanley et al, eds. *Proceedings of the NATO ARW on New kinds of phase transitions in disordered materials, Wolga River, Russia, May 24-28, 2001* (Kluwer Acad. Publ., in press)
31. C. Bennemann, W. Paul, K. Binder, B. Dünweg: *Phys. Rev.* **E57**, 843, (1998)
32. K. Binder, C. Bennemann, J. Baschnagel, W. Paul: "Anomalous diffusion of polymers in supercooled melts near the glass transition". In: R. Kutner, A. Pekalski, and K. Sznajd-Weron, eds. *Anomalous Diffusion: From Basics to Applications* (Springer, Berlin, 1999) pp. 124-139.
33. C. Bennemann, J. Baschnagel, W. Paul, K. Binder: *Comput. Theoret. Polymer Sci.* **9**, 217 (1999)
34. C. Bennemann, W. Paul, J. Baschnagel, K. Binder: *J. Phys.: Condens. Matter* **11**, 2179 (1999)
35. C. Bennemann, C. Donati, J. Baschnagel, S. C. Glotzer: *Nature* **399**, 246 (1999)
36. C. Bennemann, J. Baschnagel, W. Paul: *Eur. Phys. J.* **B10**, 323 (1999)
37. M. Aichele, J. Baschnagel: *Eur. Phys. J.* **E5**, 229, 245 (2001)
38. H.-P. Wittmann, K. Kremer, K. Binder: *J. Chem. Phys.* **96**; 6291 (1992)
39. J. Baschnagel, K. Binder, H.-P. Wittmann: *J. Phys.: Condens. Matter* **5** 1597 (1993)
40. J. Baschnagel, K. Binder: *Physica A* **204**, 47 (1994)
41. B. Lobe, J. Baschnagel: *J. Chem. Phys.* **101**, 1616 (1994)
42. J. Baschnagel: *Phys. Rev.* **49**, 135 (1994)
43. J. Baschnagel, M. Fuchs: *J. Phys.: Condens. Matter* **7**, 6761 (1995)
44. M. Wolfgardt, J. Baschnagel, K. Binder: *J. Phys. (Paris) II* **5**, 1035 (1995)
45. M. Wolfgardt, J. Baschnagel, W. Paul, K. Binder: *Phys. Rev.* **E54**, 1535 (1996)
46. K. Okun, M. Wolfgardt, J. Baschnagel, K. Binder: *Macromolecules* **30**, 3075 (1987)
47. K. Binder, J. Baschnagel, S. Böhmer, W. Paul: *Phil. Mag.* **B77**, 591 (1998)
48. V. Tries, W. Paul, J. Baschnagel, K. Binder: *J. Chem. Phys.* **106**, 738 (1997)
49. B. W. H. van Beest, G. J. Kramer, R. A. van Santen: *Phys. Rev. Lett.* **64**, 1995 (1990)
50. K. Vollmayr, W. Kob, K. Binder: *Phys. Rev.* **B54**, 15808 (1996)
51. R. Brüning, K. Samwer: *Phys. Rev.* **B46**, 11318 (1992)
52. J. Horbach, W. Kob: *Phys. Rev.* **B60**, 3169 (1999)
53. J. Horbach, W. Kob, K. Binder, A. C. Angell: *Phys. Rev.* **E54**, R5897 (1996)
54. J. Horbach, W. Kob, K. Binder: *Phil. Mag.* **B77**, 297 (1998)
55. D. L. Price, J. M. Carpenter: *J. Non-Cryst. Solids* **92**, 153 (1987)
56. J. C. Mikkelsen: *Appl. Phys. Lett.* **45**: 1187 (1984)
57. G. Brebec, R. Seguin, C. Sella, J. Bevenot, J. C. Martin: *Acta Metall.* **28**, 327 (1980)
58. T. Stühn, Diploma Thesis, University of Mainz, 2000
59. C. De Michele and F. Sciortino, preprint cond-mat/0112056.
60. D. Elderfield, D. Sherrington: *J. Phys. C: Solid State Phys.* **16**, L491, L971, L1169 (1983)
61. D. J. Gross, I. Kanter, H. Sompolinsky: *Phys. Rev. Lett* **55**, 304 (1985)
62. T. R. Kirkpatrick, P. G. Wolynes: *Phys. Rev.* **B36**, 8552 (1987)

63. T. R. Kirkpatrick, D. Thirumalai: Phys. Rev. **B37**, 5342 (1988)
64. D. Thirumalai, T. R. Kirkpatrick: Phys. Rev. **B38**, 4881 (1988)
65. G. Cwiliich, T. R. Kirkpatrick: J. Phys. A: Math. Gen **22**, 4971 (1989)
66. E. De Santis, G. Parisi, F. Ritort: J. Phys. A: Math. Gen. **28**, 3025 (1995)
67. K. Binder, A. P. Young: Rev. Mod. Phys. **58**, 801 (1986)
68. K. Kim and R. Yamamoto, Phys. Rev. E **61**, R41 (2000).
69. K. Binder: Rep. Progr. Phys. **50**, 783 (1987)
70. G. B. Mc Kenna: 'Glassformation and glassy behavior'. In: *Comprehensive Polymer Science, Vol. 2* ed. by C. Booth and C. Proce. Pergamon Press, Oxford 1986, pp. 311-362.
71. M. Doi, S. F. Edwards: *The Theory of Polymer Dynamics* (Clarendon, Oxford, 1986)
72. M. Nauroth and W. Kob, Phys. Rev. E **55**, 657 (1997).
73. G. Pezzin, F. Zilio-Grandi, P. Sanmartin: Eur. Polymer J. **6**, 1053 (1970)
74. P. J. Flory: Proc. Roy. Soc. London **A234**, 60 (1956)
75. A. Milchev: C. R. Acad. Bulg. Sci. **36**, 1415 (1983)
76. J. Baschnagel, K. Binder, W. Paul, M. Laso, U. W. Suter, I. Batoulis, W. Jilge, T. Bürger: J. Chem. Phys. **95**, 6014 (1991)
77. W. Tschöp, K. Kremer, I. Batoulis, T. Bürger, O. Hahn: Acta Polymer **49**, 61, 75 (1998)